J|A|C|S
ARTICLES
Published on Web 03/23/2004

Pyrene-Labeled Base-Discriminating Fluorescent DNA Probes for Homogeneous SNP Typing

Akimitsu Okamoto, Keiichiro Kanatani, and Isao Saito*

Contribution from the Department of Synthetic Chemistry and Biological Chemistry, Faculty of Engineering, Kyoto University and SORST, Japan Science and Technology Corporation, Kyoto 615-8510, Japan

Received November 16, 2003; E-mail: saito@sbchem.kyoto-u.ac.jp

Abstract: This paper describes the design of novel base-discriminating fluorescent (BDF) nucleobases and their application to single nucleotide polymorphism (SNP) typing. We devised novel BDF nucleosides, ^{Py}**U** and ^{Py}**C**, which contain a pyrenecarboxamide chromophore connected by a propargyl linker. The fluorescence spectrum of the duplex containing a ^{Py}**U**/A base pair showed a strong emission at 397 nm on 327 nm excitation. In contrast, the fluorescence of duplexes containing ^{Py}**U**/N base pairs (N = C, G, or T) was considerably weaker. The proposed structure of the duplex containing a matched ^{Py}**U**/A base pair suggests that the high polarity near the pyrenecarboxamide group is responsible for the strong A-selective fluorescence emission. Moreover, the fluorescence of the duplex containing a ^{Py}**U**/A base pair was not quenched by a flanking C/G base pair. The fluorescence properties are quite different from previous BDF nucleobases, where fluorescence is quenchable by flanking C/G base pairs. The duplex containing the C derivative, ^{Py}**C**, selectively emitted fluorescence when the base opposite ^{Py}**C** was G. The drastic change of fluorescence intensity by the nature of the complementary base is extremely useful for SNP typing. ^{Py}**U**- and ^{Py}**C**-containing oligodeoxynucleotides acted as effective reporter probes for homogeneous SNP typing of DNA samples containing c-Ha-*ras* and BRCA2 SNP sites.

Introduction

Fluorescence-labeled DNA probes have wide applications that range from genomic sequencing to the rapid detection of infections and genetic diseases.[1] Almost all previous assays ultimately rely upon sequence recognition events associated with DNA hybridization. For the detection of mismatched base pairs, such hybridization assays have inherent limitations in terms of their sensitivity. For example, the detection of single nucleotide alterations, such as single nucleotide polymorphisms (SNPs) and point mutations, in target sequences using a conventional hybridization assay requires a distinguishable difference in the base-pairing energies between full-matched versus mismatched sequences. These differences are usually very small when only a single mismatched base pair in an extended oligodeoxynucleotide (ODN) is involved. Furthermore, the duplex stabilities of ODNs with a fixed length sometimes vary considerably with the base content.

Fluorescence-labeled DNA probes have the potential to simplify DNA probe assays if the fluorescence label exhibits a drastic change in fluorescence intensity when the labeled probe hybridizes with a target sequence. Due to this fluorescence change, the bases on the complementary strands can be fluorometrically read out without separation and washing. We have recently demonstrated a new concept for base-discriminating fluorescent (BDF) nucleobases, which can clearly distinguish the type of base opposite the BDF base by a fluorescence change (Figure 1).[2] Although the ODNs containing BDF bases are actually used as tools for the detection of single nucleotide alterations, there are still problems to be solved, such as the quenching of the BDF fluorescence by the flanking base pairs. For example, when the flanking base pair of the BDF base, methoxybenzodeazaadenine (^{MD}A), is a G/C base pair, the fluorescence of the BDF base is considerably suppressed.[2c] A SNP typing method employing such a BDF base would be inaccurate for the sequence containing a G/C base pair near the SNP site. Thus, BDF bases that are more base-selective and insensitive to flanking base pairs are highly desirable.

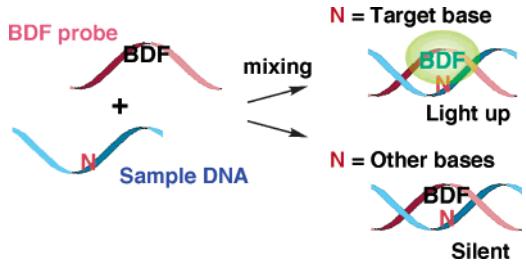

Figure 1. Schematic illustration of a new homogeneous SNP typing method using a base-discriminating fluorescent (BDF) probe. BDF probes give strong fluorescence only when the base opposite BDF base is a target base (e.g., C for ^{MD}A,[2c] T for ^{MD}I,[2c] and A for NPP[2d] and BPP[2a]).

(1) (a) Skogerboe, K. J. *Anal. Chem.* **1995**, *67*, 449R−454R. (b) Southern, E. M. *Trends Genet.* **1996**, *12*, 110−115. (c) Fodor, S. P. A. *Science* **1997**, *277*, 393. (d) Eng, C.; Vijg, J. *Nat. Biotechnol.* **1997**, *15*, 422−426.

(2) (a) Okamoto, A.; Tainaka, K.; Saito, I. *J. Am. Chem. Soc.* **2003**, *125*, 4972−4973. (b) Okamoto, A.; Tainaka, K.; Saito, I. *Chem. Lett.* **2003**, *32*, 684−685. (c) Okamoto, A.; Tanaka, K.; Fukuta, T.; Saito, I. *J. Am. Chem. Soc.* **2003**, *125*, 9296−9297. (d) Okamoto, A.; Tainaka, K.; Saito, I. *Tetrahedron Lett.* **2003**, *44*, 6871−6874.

10.1021/ja039625y CCC: $27.50

The fluorescence of pyrene-1-carboxaldehyde shows a strong dependence on the solvent polarity.[3] For example, the fluorescence in nonpolar solvents, such as *n*-hexane, is very weak ($\Phi_F < 0.001$).[3a] This particular fluorescence arises from the $n-\pi^*$ transition. However, on increasing the solvent polarity, the $\pi-\pi^*$ level, which lies close to the $n-\pi^*$ level, is lowered below the $n-\pi^*$ level during the lifetime of the excited state by solvent relaxation. Thus, in polar solvents, the $\pi-\pi^*$ state becomes a fluorescence emitting state, and pyrene-1-carboxaldehyde shows a strong fluorescence (Φ_F in ethanol = 0.15).[3a] Pyrene-1-carboxaldehyde has thus been used for probing polarity at the micelle-water interface, where it is located.[3a] Such fluorescent probes would be valuable for monitoring the microenvironment of DNA duplexes, for example, for sensing the difference in polarities between the inside and the outside of DNA duplexes. By using such fluorescence changes induced by the polarity change near the fluorophore, we propose it is feasible to experimentally sense nucleobases opposite the BDF base in a target strand. We assumed that if the pyrenecarbonyl fluorophore is attached to uracil at the C-6 position, via a rigid propargyl linker, the fluorophore would be extruded to the outside of the groove, a highly polar aqueous phase, due to base pairing with A (matched). In such a case, the pyrene-labeled BDF probe should exhibit a strong A-selective fluorescence. In contrast, when the pyrene fluorophore is intercalated into a DNA duplex due to the lack of base-pairing (mismatched), the BDF base would exhibit no emission due to the location of the fluorophore at a highly hydrophobic site in the groove. On the basis of this concept, we designed a new type of pyrene-labeled BDF nucleoside.

In this paper, we report on the synthesis and fluorescence properties of DNA probes containing a new type of pyrene-labeled BDF nucleoside. These BDF bases, **^{Py}U** and **^{Py}C**, exhibited unique fluorescence properties depending on the nature of the base on the complementary strand, and distinguished A and G opposite a BDF base, respectively, by a sharp fluorescence change. Unlike previously reported pyrene-labeled ODN probes,[4] **^{Py}U** and **^{Py}C** are the first nucleobases whose fluorescence intensities vary sharply depending on the nature of the complementary base. These **^{Py}U**- and **^{Py}C**-containing BDF probes could be effective reporter probes for homogeneous SNP typing.

Results and Discussion

Synthesis of the novel deoxyuridine-based fluorescent nucleoside is outlined in Scheme 1. 5′-protected 5-iodouridine **1** was prepared according to a method reported in the literature,[5] and then coupled with pyrene-substituted propargylamines, **5a** and **5b**, to yield compounds **2a** and **2b**, respectively. Subsequently, these were converted to phosphoramidites **3a** and **3b** for ODN synthesis. The acid hydrolysis of **2a** and **2b** afforded free nucleosides **4a** (**^{Py}U**) and **4b** (**$^{Py(amino)}$U**), respectively. ODNs containing **^{Py}U** and **$^{Py(amino)}$U** were synthesized using **3a** and **3b** according to conventional DNA synthesis.

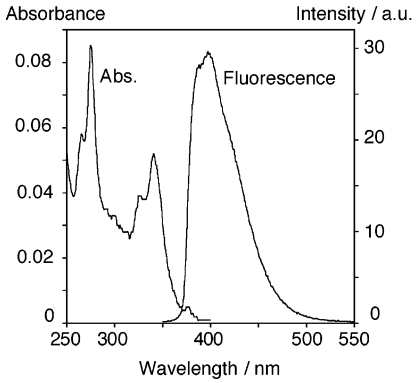

Figure 2. Absorption and fluorescence spectra of 2.5 μM **^{Py}U** monomer (50 mM sodium phosphate, 0.1 M sodium chloride, pH = 7.0, 25 °C). Excitation wavelength was 345 nm. λ_{max} = 341 nm (ϵ 20,800). λ_{em} = 397 nm. Φ_F = 0.209.

Scheme 1 [a]

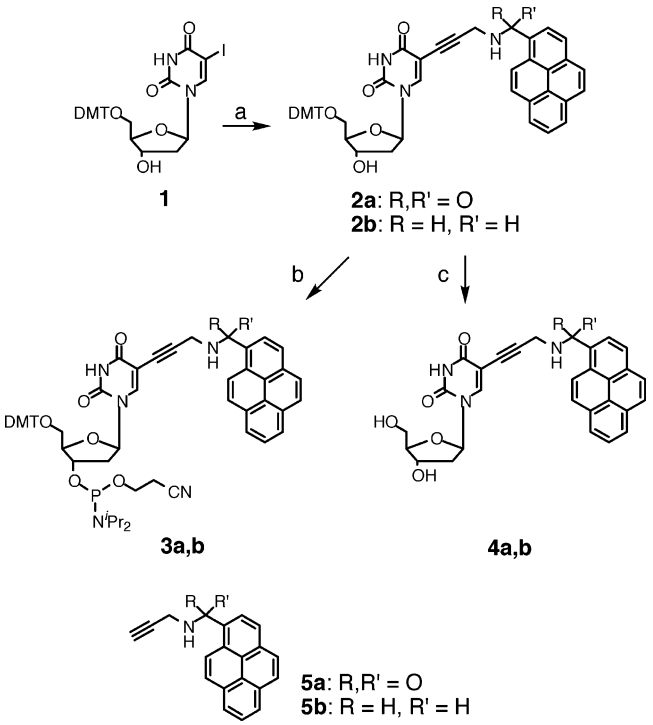

[a] Reagents and conditions: (a) **5a** or **5b**, $Pd(Ph_3P)_4$, CuI, triethylamine, *N*,*N*-dimethylformamide, room temperature, 12 h, 60% for **2a**, 60% for **2b**; (b) $(^iPr_2N)_2PO(CH_2)_2CN$, 1*H*-tetrazole, acetonitrile, room temperature, 1 h, *quant*.; (c) trichloroacetic acid, dichloromethane, room temperature, 5 min, 27% for **4a**, 75% for **4b**.

First, the absorption and fluorescence spectra of nucleoside **^{Py}U** were measured in sodium phosphate buffer (pH = 7.0) (Figure 2). The absorption maximum λ_{max} of **^{Py}U** was observed at 341 nm, characteristic of the pyrene chromophore. A strong fluorescence at 397 nm was observed on excitation at 345 nm (Φ_F = 0.209).

Before measuring the absorption and fluorescence of **^{Py}U**-containing ODN, we examined the duplex stabilities of **^{Py}U**-containing ODN 5′-d(CGCAAT**^{Py}U**TAACGC)-3′ (**ODN1-(^{Py}U)**) hybridized with complementary strand 5′-d(GC-

(3) (a) Kalyanasundaram, K.; Thomas, J. K. *J. Phys. Chem.* **1977**, *81*, 2176−2180. (b) de Silva, A. P.; Gunaratne, H. Q. N.; Gunnlaugsson, T.; Huxley, A. J. M.; McCoy, C. P.; Rademacher, J. T.; Rice, T. E. *Chem. Rev.* **1997**, *97*, 1515−1566.
(4) (a) Mann, J. S.; Shibata, Y.; Meehan, T. *Bioconjugate Chem.* **1992**, *3*, 554−558. (b) Korshun, V. A.; Prokhorenko, I. A.; Gontarev, S. V.; Skorobogatyi, M. V.; Balakin, K. V.; Manasova, E. V.; Malakhov, A. D.; Berlin, Y. A. *Nucleosides & Nucleotides* **1997**, *16*, 1461−1464. (c) Lewis, F. D.; Zhang, Y.; Letsinger, R. L. *J. Am. Chem. Soc.* **1997**, *119*, 5451−5452. (d) Paris, P. L.; Langenhan, J. M.; Kool, E. T. *Nucleic Acids Res.* **1998**, *26*, 3789−3793. (e) Yamana, K.; Zako, H.; Azuma, K.; Iwase, R.; Nakano, H.; Murakami, A. *Angew. Chem., Int. Ed.* **2001**, *40*, 1104−1106. (f) Amann, N.; Pandurski, E.; Fiebig, E.; Wagenknecht, H.-A. *Chem. Eur. J.* **2002**, *8*, 4877−4883.
(5) Sheardy, R. D.; Seeman, N. C. *J. Org. Chem.* **1986**, *51*, 4301−4303.

Table 1. Melting Temperatures and Photophysical Properties of Pyrene-Labeled ODNs[a]

sequences[b]	N	T_m/°C	λ_{max}/nm	ϵ_{max}	ϵ [c]	λ_{em}/nm	Φ_F [d]
ODN1(^{Py}U)			350	20 400	11 600 (327)	402	0.077
ODN1(^{Py}U)/ODN1′(N)	A	49.8	342	23 200	16 400 (327)	397	0.203
	C	42.5	350	18 800	10 800 (327)	395	0.136
	G	42.5	350	18 000	9 600 (327)	399	0.070
	T	40.8	350	13 200	8 800 (327)	393	0.045
ODN1($^{Py(amino)}$U)			335, 351	18 800, 26 800	25 200 (350)	380, 397	0.0015
ODN1($^{Py(amino)}$U)/ODN1′(N)	A	58.2	336, 353	21 200, 26 800	24 000 (350)	381, 396	0.0010
	C	51.2	335, 352	18 000, 23 600	22 000 (350)	380, 397	0.0014
	G	49.1	335, 352	20 400, 25 600	24 000 (350)	381, 397	0.0011
	T	53.2	335, 352	19 200, 24 000	22 400 (350)	381, 396	0.0004
ODN2(^{Py}U)			350	22 800	20 400 (344)	399	0.048
ODN2(^{Py}U)/ODN2′(N)	A	58.9	343	24 800	24 800 (344)	395	0.151
	C	51.2	350	21 600	18 400 (344)	399	0.023
	G	50.4	350	20 400	17 600 (344)	400	0.029
	T	49.9	350	19 200	17 200 (344)	396	0.035
ODN2(^{Py}C)			350	18 400	13 600 (329)	400	0.068
ODN2(^{Py}C)/ODN2′(N)	A	57.9	350	21 600	17 200 (329)	403	0.035
	C	50.0	350	17 200	11 600 (329)	400	0.016
	G	65.1	343	20 800	16 000 (329)	393	0.147
	T	55.5	350	18 400	14 000 (329)	401	0.027

[a] The duplexes (2.5 μM) were measured in 50 mM sodium phosphate and 0.1 M sodium chloride (pH = 7.0) at 25 °C. [b] **ODN1(^{Py}U)** = 5′-d(CGCAAT^{Py}UTAACGC)-3′, **ODN1′(N)** = 5′-d(GCGTTANATTGCG)-3′ (**N** = A, C, G or T), **ODN1($^{Py(amino)}$U)** = 5′-d(CGCAAT$^{Py(amino)}$UTAACGC)-3′, **ODN2(^{Py}U)** = 5′-d(CGCAAC^{Py}UCAACGC)-3′, **ODN2′(N)** = 5′-d(GCGTTGNGTTGCG)-3′ (**N** = A, C, G or T), **ODN2(^{Py}C)** = 5′-d(CGCAAC^{Py}C-CAACGC)-3′. [c] ϵ is the molar extinction coefficient given at the wavelength shown in parentheses, which are the excitation wavelength in fluorescence measurements. [d] The fluorescence quantum yields (Φ_F) were calculated according to ref 6.

GTTA**N**ATTGCG)-3′ (**ODN1′(N)**, **N** = A, C, G, or T) (Table 1). The melting temperature of **ODN1(^{Py}U)/ODN1′(A)** was 7 to 9 °C higher than that observed for other mismatched duplexes in sodium phosphate buffer (pH 7.0). The high stability of duplex **ODN1(^{Py}U)/ODN1′(A)** suggests that **^{Py}U** forms a stable base pair only with A.

Measurements of the absorption and fluorescence spectra of 2.5 μM of **ODN1(^{Py}U)/ODN1′(N)** duplex in sodium phosphate buffer (pH = 7.0) were performed. The results are summarized in Figure 3 and Table 1. The absorption maximum λ_{max} of the matched duplex **ODN1(^{Py}U)/ODN1′(A)** was 342 nm, which was close to the λ_{max} observed for **^{Py}U** nucleoside (Figure 3a). In contrast, when the complementary base of **^{Py}U** was a mismatched base (i.e., **N** = C, G, and T), the absorption maximum was at 350 nm, which was 9 nm higher than that of the **^{Py}U** nucleoside. The absorption data suggests that the pyrenecarboxamide chromophore of **ODN1(^{Py}U)/ODN1′(N)** duplexes, except for that of **ODN1(^{Py}U)/ODN1′(A)**, strongly interacts with the duplex strand. The fluorescence spectrum of **ODN1(^{Py}U)/ODN1′(A)** showed a strong fluorescence at 397 nm at 327 nm excitation (Φ_F = 0.203). In contrast to the high fluorescence intensity for full-matched duplex, the fluorescence of single-stranded **ODN1(^{Py}U)** and mismatched **ODN1(^{Py}U)/ODN1′(N)** duplexes was much weaker. The fluorescence excitation spectra exhibited strong peaks arising from **^{Py}U** in the duplexes (Figure 3b). This suggests that the change in microenvironment near the pyrenecarboxamide chromophore of **^{Py}U** in each duplex would lead to these remarkable differences in fluorescence intensities.

The fluorescence of pyrene-1-carboxaldehyde is known to be highly dependent on the solvent polarity.[3,7] The fluorescence intensity of pyrene-1-carboxaldehyde is very strong in polar solvents due to the preferred $\pi-\pi^*$ transition. In nonpolar solvents, a weak fluorescence, attributed to a nonemissive $n-\pi^*$ transition, is observed.[7b,8] We examined the effect of solvent on the fluorescence of **^{Py}U** nucleoside **4a**. The quantum yield of **4a** increased with increasing solvent polarity (Φ_F = 0.068 in carbon tetrachloride and 0.211 in methanol). In contrast, the fluorescence of **$^{Py(amino)}$U** nucleoside **4b**, which does not possess an amide carbonyl group, was very weak, and little affected by the solvent polarity (Φ_F = 0.027 in carbon tetrachloride and 0.057 in methanol). This fluorescence behavior indicates that the pyrenecarboxamide chromophore of **^{Py}U** can act as an antenna that is highly sensitive to the solvent polarity. The fluorescence change of **$^{Py(amino)}$U**-containing duplexes **ODN1($^{Py(amino)}$U)/ODN1′(N)** was also examined (Figure 4). The fluorescence quantum yields were very low (Φ_F < 0.002), and the selectivity of **ODN1($^{Py(amino)}$U)/ODN1′(N)** against the four bases (**N** = A, C, G and T) was also very low. The results obtained from comparative experiments using **^{Py}U** and **$^{Py(amino)}$U** clearly indicate that the base-selective fluorescence emission by **ODN1(^{Py}U)** strongly correlates with the polarity sensitivity of the **^{Py}U** fluorophore.

To confirm the proposed principle of A-selective fluorescence emission of **^{Py}U**, we performed a molecular modeling study of the **^{Py}U**-containing duplexes (Figure 5). The structure of the **^{Py}U**-containing duplexes was obtained from optimization of 5′-d(AAAC**^{Py}U**CAAA)-3′/5′-d(TTTG**N**GTTT)-3′ (**N** = A or G) using the AMBER* force field in water employing MacroModel (ver. 6.0). In the energy-minimized structures for the duplex containing a **^{Py}U**/A base pair, the pyrenecarboxamide chromophore of **^{Py}U** was extruded to the outside of the duplex, and exposed to a highly polar aqueous phase, as shown in Figure 5a. In contrast, the duplex containing a **^{Py}U**/G mismatched base pair showed a structure in which the glycosyl bond of uridine was rotated to the syn conformation, as shown in Figure 5b. The propargyl linker of **^{Py}U** was stacked into the minor groove

(6) Morris, J. V.; Mahaney, M. A.; Huber, J. R. *J. Phys. Chem.* **1976**, *80*, 969−974.

(7) (a) Lianos, P.; Cremel, G. *Photochem. Photobiol.* **1980**, *31*, 429−434. (b) Kumar, C. V.; Chattopadhyay, S. K.; Das, P. K. *Photochem. Photobiol.* **1983**, *38*, 141−152. (c) Cundall, R. B. *Photochemistry* **1992**, *23*, 3−8. (d) Ahuja, R. C.; Moebius, D. *Langmuir* **1992**, *8*, 1136−1144.

(8) Murov. S. L.; Carmichael, I.; Hug, G. L. *Handbook of Photochemistry*, 2nd ed.; Marcel Dekker: New York, 1993.

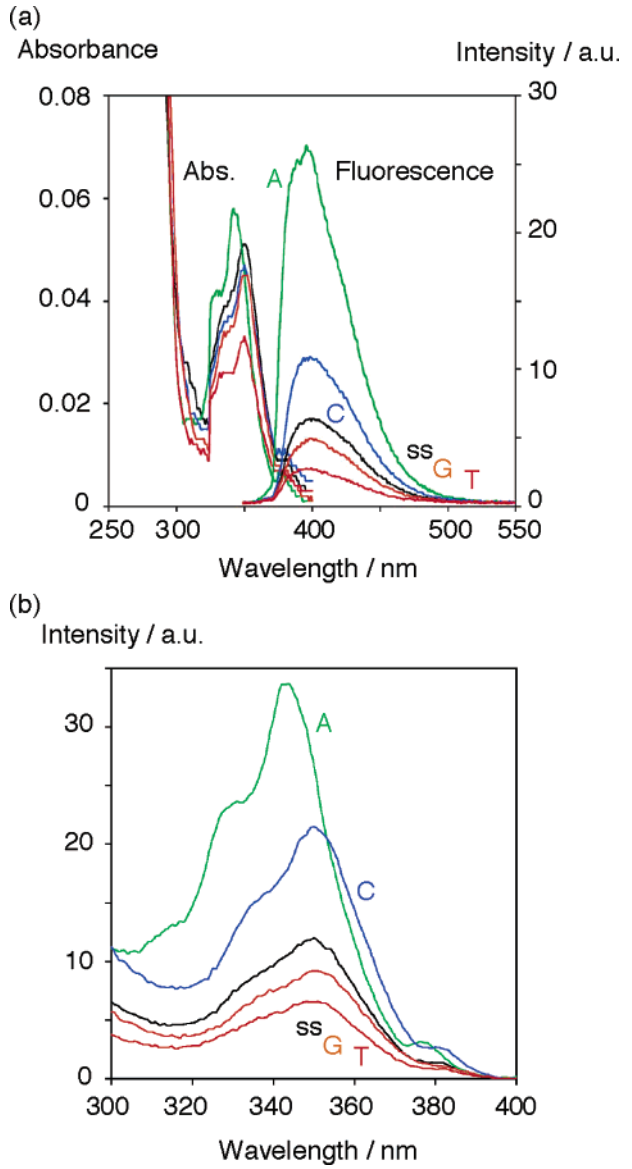

Figure 3. Spectral change of 2.5 μM **ODN1(**^{Py}**U)** hybridized with 2.5 μM **ODN1′(N)** (**N** = A, C, G, or T) (50 mM sodium phosphate, 0.1 M sodium chloride, pH = 7.0, 25 °C). "ss" denotes single-stranded **ODN1(**^{Py}**U)**. (a) Absorption and fluorescence spectra. Excitation wavelength was 327 nm. (b) Fluorescence excitation spectra for 347 nm emission.

and the pyrenecarboxamide unit was bound to the duplex along the minor groove. In this conformation, the pyrenecarboxamide group was located at a hydrophobic site of the duplex. The polarity of the microenvironments near the ^{Py}**U** pyrenecarboxamide group in both cases was quite different. Thus, our modeling study suggests that the polarity difference around the pyrenecarboxamide group of ^{Py}**U** directly contributed to the A-selective fluorescence emission of **ODN1(**^{Py}**U)/ODN1′(N)** duplexes.

Next, we examined the effect of the flanking base pair on the fluorescence intensity. The C/G base pair is well-known to stabilize intercalated structures.[9] The stacking of the flanking C/G base pair to ^{Py}**U**, and particularly to the ^{Py}**U** side chain-intercalating structure, may be the reason for the duplex stabilization (Figure 4b). Therefore, to investigate the effect of

(9) (a) Nakatani, K.; Okamoto, A.; Matsuno, T.; Saito, I. *J. Am. Chem. Soc.* **1998**, *120*, 11 219−11 225. (b) Nakatani, K.; Sando, S.; Saito, I. *Nat. Biotechnol.* **2001**, *19*, 51−55.

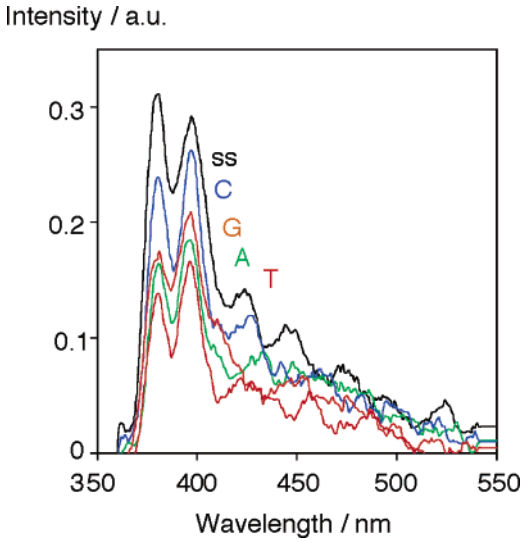

Figure 4. Fluorescence spectra of 2.5 μM **ODN1(**$^{Py(amino)}$**U)** hybridized with 2.5 μM **ODN1′(N)** (**N** = A, C, G, or T) (50 mM sodium phosphate, 0.1 M sodium chloride, pH = 7.0, 25 °C). Excitation wavelength was 350 nm.

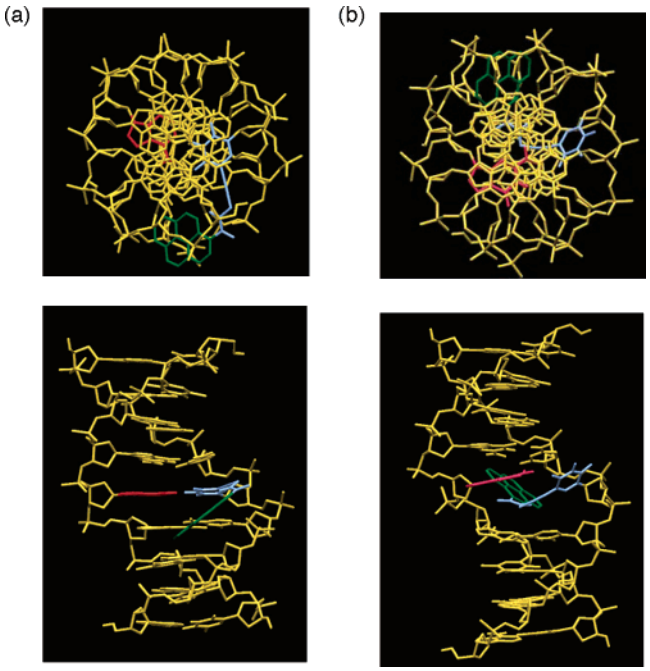

Figure 5. Molecular modeling of the simulated conformations of duplexes 5′-d(AAAC^{Py}**U**CAAA)-3′/5′-d(TTTG**N**GTTT)-3′ (**N** = A or G). The models were optimized by AMBER* force field in water using MacroModel version 5.0. Top views (top) and side views from the major groove (bottom) are shown. ^{Py}**U** and complementary **N** base are represented by blue and red, respectively. Pyrene group of ^{Py}**U** is shown in green. (a) **N** = A. (b) **N** = G.

the flanking base pair on the fluorescence emission, we prepared a BDF probe containing the −C^{Py}**U**C− sequence, 5′-d(CGCAAC^{Py}**U**CAACGC)-3′ (**ODN2(**^{Py}**U)**), and measured the fluorescence of duplexes hybridized with the complementary strand 5′-d(GCGTTG**N**GTTGCG)-3′ (**ODN2′(N)**, **N** = A, C, G, or T). The fluorescence quantum yield of **ODN2(**^{Py}**U)/ODN2′(A)** was relatively high (Φ_F = 0.151), whereas the fluorescence emissions of the single-stranded **ODN2(**^{Py}**U)** and duplex **ODN2(**^{Py}**U)/ODN2′(N)** were strongly suppressed (Figure 6). The fluorescence of **ODN2(**^{Py}**U)/ODN2′(N)** was more A-selective than **ODN1(**^{Py}**U)/ODN1′(N)**. These results suggest that the ^{Py}**U**

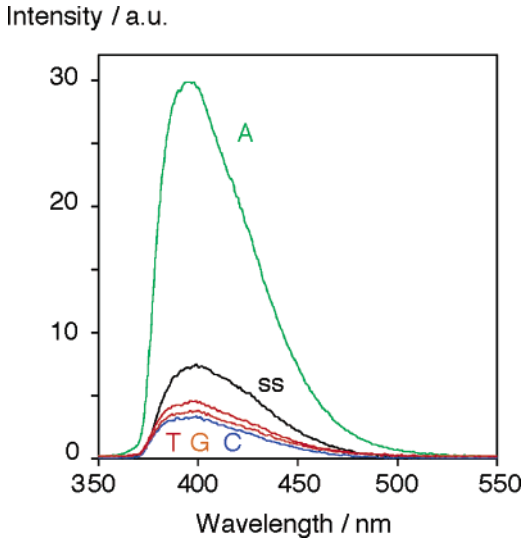

Figure 6. Fluorescence spectra of 2.5 μM **ODN2(**^{Py}**U)** hybridized with 2.5 μM **ODN2′(N)** (**N** = A, C, G, or T) (50 mM sodium phosphate, 0.1 M sodium chloride, pH = 7.0, 25 °C). Excitation wavelength was 344 nm

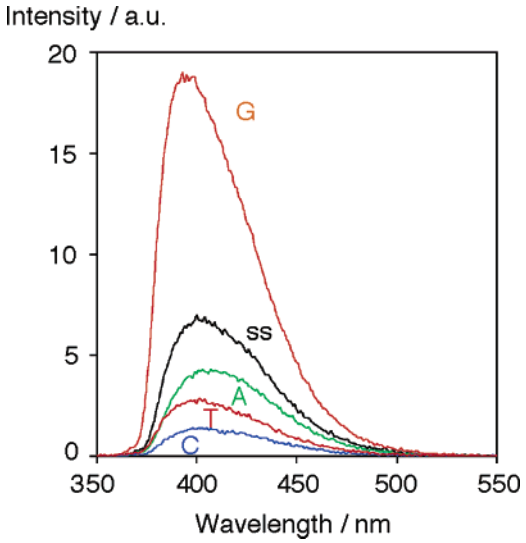

Figure 7. Fluorescence spectra of 2.5 μM **ODN2(**^{Py}**C)** hybridized with 2.5 μM **ODN2′(N)** (**N** = A, C, G, or T) (50 mM sodium phosphate, 0.1 M sodium chloride, pH = 7.0, 25 °C). Excitation wavelength was 329 nm.

Scheme 2 [a]

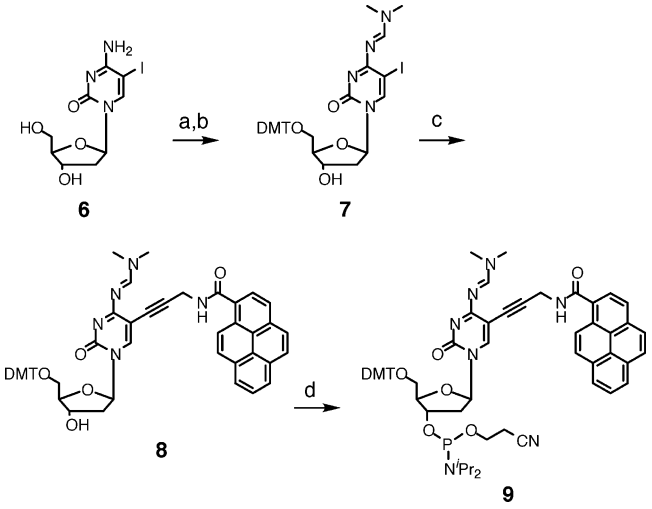

[a] Reagents and conditions: (a) *N*,*N*-dimethylformamide dimethylacetal, *N*,*N*-dimethylformamide, 55 °C, 2 h; (b) 4,4′-dimethoxytrityl chloride, pyridine, room temperature, 5 h, 50% (two steps); (c) **5a**, $Pd(Ph_3P)_4$, CuI, triethylamine, *N*,*N*-dimethylformamide, room temperature, 12 h, 47%; (d) $(^iPr_2N)_2PO(CH_2)_2CN$, 1*H*-tetrazole, acetonitrile, room temperature, 1 h, *quant*.

side chain-intercalating conformation in the mismatched duplexes was stabilized by the flanking C/G base pair, resulting in a suppression of their fluorescence intensity. In addition, it should be noted that the fluorescence of **ODN2(**^{Py}**U)/ODN2′-(A)** was not quenched by the flanking C/G base pair. These fluorescence properties are quite different from those observed in previous BDF nucleobases,[2] where the fluorescence is efficiently quenched by flanking C/G base pairs.

Since ^{Py}**U** shows a highly A-selective fluorescence emission, we expected that the analogous C derivative (^{Py}**C**) would exhibit a G-selective fluorescence emission. Thus, we prepared ^{Py}**C** according to Scheme 2, and measured the absorption and fluorescence spectra of the ^{Py}**C**-containing ODN, 5′-d(CGCAAC^{Py}**C**CAACGC)-3′ (**ODN2(**^{Py}**C)**), hybridized with the complementary strand **ODN2′(N)** (Figure 7). The absorption maxima λ_{max} of **ODN2(**^{Py}**C)/ODN2′(N)** were 343 nm for matched (**N** = G) and 350 nm for mismatched bases. These results are similar to the absorption behavior of ^{Py}**U**-containing ODN duplexes. The fluorescence emission from **ODN2(**^{Py}**C)/ODN2′(N)** was highly G-selective, as shown in Figure 6. BDF nucleoside that emits fluorescence selectively for G is unusual, and ^{Py}**C** is the first BDF nucleoside that can detect G base on the complementary strand.

The fluorescence change induced by the nature of a complementary base would be very useful for SNP typing. Therefore, we examined the discrimination of SNPs in human SNP sequences using ^{Py}**U**- and ^{Py}**C**-containing BDF probes. 15-mer DNA strands containing c-Ha-*ras*[10] and BRCA2 SNP sites[11] were used as target sequences (Figure 8). For the *ras* gene c-Ha-*ras* sequence, which possesses a C/A SNP site, we designed a ^{Py}**U**-containing BDF probe, 5′-d(GGCGCCG^{Py}**U**CGGTGTG)-3′ (**ODN$_{ras}$(**^{Py}**U)**). On hybridization with the target sequence, **ODN$_{ras}$(**^{Py}**U)** showed an A-allele-specific fluorescence at 398 nm using an excitation wavelength of 344 nm, as shown in Figure 8a and Table 2. The fluorescence of a nonhybridized ODN or an ODN probe hybridized with a C-allele sequence was negligible. Similarly, for a BRCA2 sequence possessing a T/G SNP site, the ^{Py}**C**-containing BDF probe, 5′-d(GCAGCCT^{Py}**C**AGGCAGC)-3′ (**ODN$_{BRCA2}$(**^{Py}**C)**), was prepared. The fluorescence of **ODN$_{BRCA2}$(**^{Py}**C)** hybridized with the target sequence was highly G-allele-selective (Figure 8b and Table 3). Thus, these BDF probes act as effective fluorescence probes for the detection of single nucleotide alterations. The difference in fluorescence intensities was more conveniently and precisely detectable using a fluorescence imager, as shown in Figure 8. The use of ^{Py}**U**- and ^{Py}**C**-containing BDF probes made it possible to judge the type of base located at a specific site on the target DNA by simple mixing.

(10) Reddy, E. P.; Reynold, R. K.; Santo, E.; Barbacid, M. *Nature* **1982**, *300*, 149−152.
(11) Ford, D.; Easton, D. F.; Stratton, M.; Narod, S.; Goldgar, D.; Devilee, P.; Bishop, D. T.; Weber, B.; Lenoir, G.; Chang-Claude, J.; Sobol, H.; Teare, M. D.; Struewing, J.; Arason, A.; Scherneck, S.; Peto, J.; Rebbeck, T. R.; Tonin, P.; Neuhausen, S.; Barkardottir, R.; Eyfjord, J.; Lynch, H.; Ponder, B. A. J.; Gayther, S. A.; Birch, J. M.; Lindblom, A.; Stoppa-Lyonnet, D.; Bignon, Y.; Borg, A.; Hamann, U.; Haites, N.; Scott, R. J.; Maugard, C. M.; Vasen, H.; Seitz, S.; Cannon-Albright, L. A.; Schofield, A.; Zelada-Hedman, M. *Am. J. Hum. Genet.* **1998**, *62*, 676−689.

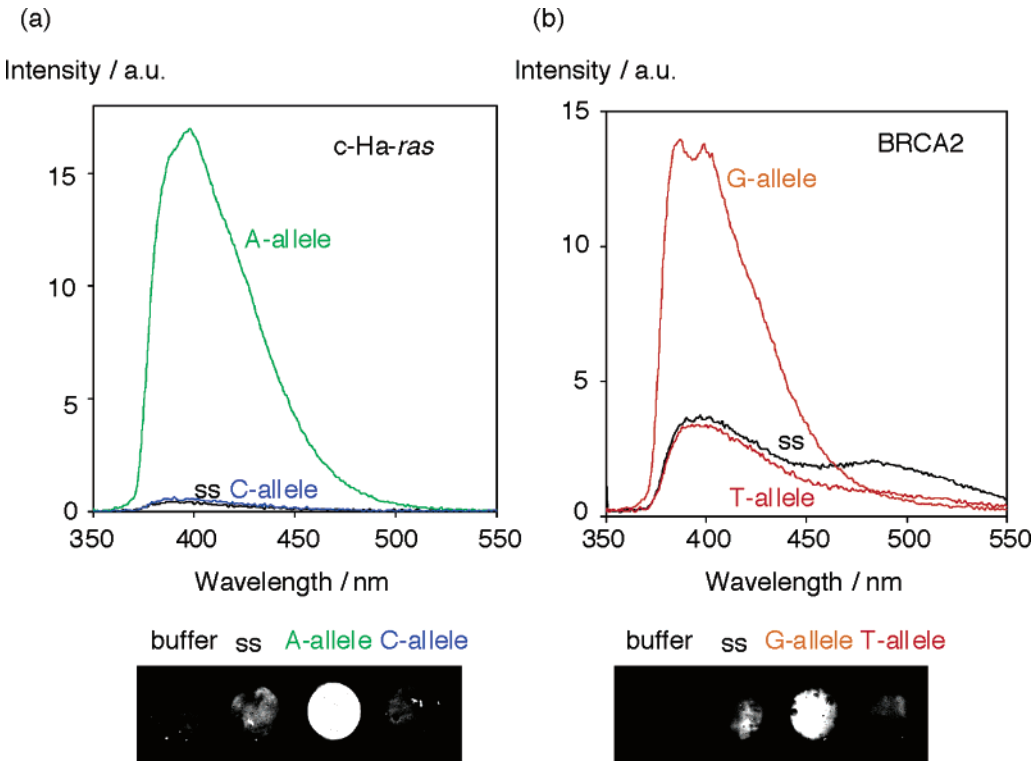

Figure 8. Fluorescence spectra (top) and images (bottom) of 15-mer SNP sequences of human gene hybridized with ^{Py}**U**- or ^{Py}**C**-containing BDF probes. (a) c-Ha-*ras* C/A SNP sequence (2.5 μM) was hybridized with 2.5 μM **ODN$_{ras}$(^{Py}U)** (50 mM sodium phosphate, 0.1 M sodium chloride, pH = 7.0, 25 °C). Excitation wavelength was 344 nm. "ss" denotes single-stranded **ODN$_{ras}$(^{Py}U)**. For fluorescence imaging, the sample solutions were illuminated with a UV transilluminator (290−365 nm). The image was taken through a 380-nm long pass emission filter by means of CCD camera. (b) BRCA2 T/G SNP sequence (2.5 μM) was hybridized with 2.5 μM **ODN$_{BRCA2}$(^{Py}C)** (50 mM sodium phosphate, 0.1 M sodium chloride, pH = 7.0, 25 °C). Excitation wavelength was 345 nm. "ss" denotes single-stranded **ODN$_{BRCA2}$(^{Py}C)**. For fluorescence imaging, the sample solutions were illuminated under a UV transilluminator (290−365 nm). The image was taken as described above.

Table 2. Photophysical Properties of BDF Probe ODN$_{ras}$(^{Py}U) Hybridized to c-Ha-*ras* SNP Sequence[a,b]

allele	λ_{max} (nm)	$\epsilon_{\lambda max}$	ϵ_{344}	λ_{em} (nm)[c]	Φ_F[c]
probe only	350	17 200	14 800	392	0.004
C	350	17 200	14 000	390	0.006
A	344	21 200	21 200	398	0.101

[a] **ODN$_{ras}$(^{Py}U)** = 5′-d(GGCGCCG^{Py}UCGGTGTG)-3′, c-Ha-*ras* SNP sequence = 5′-d(CACACCGNCGGCGCC)-3′ (**N** = C or A). [b] 2.5 μM duplex in 50 mM sodium phosphate, 0.1 M sodium chloride (pH = 7.0) at 25 °C. [c] λ_{ex} = 344 nm. The fluorescence quantum yields (Φ_F) were calculated according to ref 6.

Table 3. Photophysical Properties of BDF Probe ODN$_{BRCA2}$(^{Py}C) Hybridized to BRCA2 SNP Sequence[a,b]

allele	λ_{max} (nm)	$\epsilon_{\lambda max}$	ϵ_{345}	λ_{em} (nm)[c]	Φ_F[c]
probe only	351	17 200	16 400	387	0.035
T	351	21 200	20 000	390	0.028
G	346	16 800	16 800	390	0.107

[a] **ODN$_{BRCA2}$(^{Py}C)** = 5′-d(GCAGCCT^{Py}CAGGCAGC)-3′, BRCA2 SNP sequence = 5′-d(GCTGCCTNAGGCTGC)-3′ (**N** = T or G). [b] 2.5 μM duplex in 50 mM sodium phosphate, 0.1 M sodium chloride (pH = 7.0) at 25 °C. [c] λ_{ex} = 345 nm. The fluorescemce quantum yields (Φ_F) were calculated according to ref 6.

Conclusions

We have devised novel pyrene-labeled BDF nucleosides, ^{Py}**U** and ^{Py}**C**. BDF probes containing these fluorescent nucleosides selectively emit fluorescence when the complementary bases are A and G, respectively. Furthermore, the fluorescence of ^{Py}**U** and ^{Py}**C** is not quenched by the flanking base pairs, which is quite different from the previously observed behavior of BDF nucleosides.[2] The homogeneous SNP typing method using ^{Py}**U**- and ^{Py}**C**-containing BDF probes would be a powerful alternative to conventional SNP typing methods.

Experimental Section

General. ^{1}H NMR spectra were measured with Varian Mercury 400 (400 MHz) and JEOL JMN α-500 (500 MHz) spectrometers. ^{13}C NMR spectra were measured with JEOL JMN α-500 (125 MHz) spectrometer. Coupling constant (*J* value) are reported in hertz. The chemical shifts are shown in ppm downfield from tetramethylsilane, using residual chloroform (δ = 7.24 in ^{1}H NMR, δ = 77.0 in ^{13}C NMR), dimethyl sulfoxide (δ = 2.48 in ^{1}H NMR, δ = 39.5 in ^{13}C NMR), and methanol (δ = 3.30 in ^{1}H NMR, δ = 49.0 in ^{13}C NMR), as an internal standard. FAB masses were recorded on a JEOL JMS HX-110A spectrometer. ESI masses were recorded on a Perseptive Mariner ESI-TOF mass spectrometer.

The reagents for DNA synthesis were purchased from Glen Research. Masses of oligodeoxynucleotides were determined with a MALDI-TOF MS (Perseptive Voyager Elite, acceleration voltage 21 kV, negative mode) with 2′,3′,4′-trihydroxyacetophenone as a matrix, using T_8 ([M−H]$^-$ 2370.61) and T_{17} ([M−H]$^-$ 5108.37) as an internal standard for oligodeoxynucleotides. Calf intestinal alkaline phosphatase (Promega), Crotalus adamanteus venom phosphodiesterase I (USB), and *Penicillium citrinum* nuclease P1 (Roche) were used for the enzymatic digestion of ODNs. All aqueous solutions utilized purified water (Millipore, Milli-Q sp UF). Reversed-phase HPLC was performed on CHEMCO-BOND 5-ODS−H columns (10 × 150 mm, 4.6 × 150 mm) with a Gilson Chromatograph, Model 305, using a UV detector, Model 118, at 254 or 360 nm.

***N*-Propargyl-1-pyrenecarboxamide (5a).** A solution of 1-pyrenecarboxylic acid (500 mg, 2.03 mmol) and EDCI (388 mg, 2.03 mmol)

in anhydrous DMF (10 mL) was stirred at room temperature. After 15 min, propargylamine (0.139 mL, 2.03 mmol) was added, and the mixture was stirred at room temperature for 2.5 h. The resulting mixture was concentrated in vacuo and diluted with ethyl acetate. This solution was washed with sat. NH_4Cl solution and brine, dried over $MgSO_4$, filtered and evaporated. The crude product was purified by silica gel column chromatography (chloroform−methanol = 30:1) to yield 5a (500 mg, 87%) as a yellow solid: ^{1}H NMR ($CDCl_3$, 400 MHz) δ = 8.62 (d, 1H, J = 9.3 Hz), 8.25 (d, 1H, J = 7.6 Hz), 8.26−8.04 (7H), 6.30 (br, 1H), 4.45 (dd, 2H, J = 5.2, 2.6 Hz), 2.35 (t, 1H, J = 2.6 Hz); ^{13}C NMR (DMSO-d_6, 125 MHz) δ = 169.5, 132.8, 131.1, 130.6, 128.9, 128.84, 128.81, 127.0, 126.4, 125.9, 125.8, 124.7, 124.5, 124.30, 124.26, 124.2, 79.4, 72.1, 30.0; FABMS (NBA/$CDCl_3$), m/z 283 (M^+), HRMS calcd. for $C_{20}H_{13}NO$ (M^+) 283.0997, found 283.0996.

***N*-(1-Pyrenylmethyl)propargylamine (5b).** To a solution of pyrenecarboxaldehyde (1.00 g, 4.34 mmol) and propargylamine (0.365 mL, 5.21 mmol) in methanol (10 mL) was added sodium cyanoborohydride (327 mg, 5.21 mmol). The mixture was stirred at room temperature for 1 h. The resulting mixture was concentrated and diluted in ethyl acetate. This solution was washed with *sat.* NH_4Cl and *sat.* $NaHCO_3$, dried over Na_2SO_4, filtered and evaporated. The crude product was purified by silica gel column chromatography (chloroform-methanol = 50:1) to yield **5b** (901 mg, 77%) as a white solid: ^{1}H NMR ($CDCl_3$, 400 MHz) δ = 8.42−7.97 (9H), 4.58 (s, 2H), 3.56 (s, 2H), 2.39 (t, 1H, J = 2.2 Hz); ^{13}C NMR (DMSO-d_6, 125 MHz) δ = 133.8, 130.7, 130.3, 129.9, 128.7, 127.3, 127.2, 127.0, 126.7, 126.0, 124.94, 124.90, 124.5, 124.1, 123.9, 123.7, 82.9, 73.9, 49.2, 37.1; FABMS (NBA/$CDCl_3$), m/z 269 (M^+), HRMS calcd. for $C_{20}H_{15}N$ (M^+) 269.1204, found 269.1204.

5-[3-(1-Pyrenecarboxamido)propynyl]-5′-*O*-(4,4′-dimethoxytrityl)-2′-deoxyuridine (2a). To a solution of 5-iodo-5′-*O*-(4,4′-dimethoxytrityl)-2′-deoxyuridine[5] (**1**, 523 mg, 0.961 mmol), **5a** (323 mg, 1.24 mmol), and triethylamine (0.53 mL, 3.79 mmol) in 10 mL of anhydrous DMF was added tetrakis(triphenylphosphine)palladium(0) (492 mg, 0.426 mmol) and copper(I) iodide (162 mg, 0.852 mmol) under nitrogen. The mixture was stirred at room temperature for 12 h. The resulting mixture was concentrated in vacuo and diluted with ethyl acetate. This solution was washed with 5% (w/v) EDTA solution and 5% (w/v) sodium bisulfite solution, dried over Na_2SO_4, filtered and evaporated. The crude product was purified by silica gel column chromatography (chloroform−methanol = 50:1) to yield **2a** (465 mg, 60%) as a yellow solid: ^{1}H NMR (DMSO-d_6, 400 MHz) δ = 11.70 (br, 1H), 9.13 (t, 1H, J = 5.5 Hz), 8.51 (d, 1H, J = 5.6 Hz), 8.37−8.08 (8H), 7.96 (s, 1H), 7.42−7.20 (9H), 6.88 (dd, 4H, J = 9.2, 3.2 Hz), 6.11 (t, 1H, J = 6.8 Hz), 5.33 (d, 1H, J = 4.4 Hz), 4.29 (d, 2H, J = 4.8 Hz), 3.93−3.90 (m, 1H), 3.73 (s, 1H), 3.69 (s, 3H), 3.68 (s, 3H), 3.28−3.24 (m, 1H), 3.07 (dd, 1H, J = 10.3, 2.7 Hz), 2.29 (dt, 1H, J = 13.2, 6.4 Hz), 2.19 (ddd, 1H, J = 13.6, 6.4, 3.5 Hz); ^{13}C NMR (DMSO-d_6, 125 MHz) δ = 168.4, 161.6, 158.1, 158.0, 149.3, 144.8, 143.2, 135.6, 135.2, 131.7, 131.0, 130.7, 130.1, 129.71, 129.65, 129.59, 128.3, 128.1, 127.90, 127.85, 127.5, 127.1, 126.6, 126.5, 125.8, 125.6, 125.2, 124.6, 124.3, 123.74, 123.56, 113.23, 113.19, 98.3, 89.6, 85.9, 85.8, 85.0, 79.1, 74.1, 70.5, 63.7, 55.0, 54.9, 29.4; FABMS (NBA/DMSO), m/z 811 (M^+), HRMS calcd. for $C_{50}H_{41}N_3O_8$ (M^+) 811.2894, found 811.2883.

5-[3-(1-Pyrenecarboxamido)propynyl]-5′-*O*-(4,4′-dimethoxytrityl)-2′-deoxyuridine 3′-*O*-(2-cyanoethyl)-*N*,*N*-diisopropylphosphoramidite (3a). To a solution of **2a** (57 mg, 70 μmol) and tetrazole (5.4 mg, 77 μmol) in anhydrous acetonitrile (0.8 mL) was added 2-cyanoethyl tetraisopropylphosphorodiamidite (25 μL, 77 μmol) under nitrogen. The mixture was stirred at room temperature for 1h. The mixture was filtered and used for oligodeoxynucleotide synthesis without further purification.

5-[3-(1-Pyrenecarboxamido)propynyl]-2′-deoxyuridine (4a). To a solution of **2a** (70 mg, 86.2 μmol) in 1 mL of dichloromethane was added 3% trichloroacetic acid in dichloromethane (2 mL) and the mixture was stirred for 5 min at room temperature. The resulting mixture was evaporated and purified by recycling preparative HPLC (JAIST LC-908, JAIGEL GS-310, methanol) to yield **4a** (12 mg, 27%): ^{1}H NMR (DMSO-d_6, 500 MHz) δ = 11.63 (br, 1H), 9.22 (t, 1H, J = 5.6 Hz), 8.53 (d, 1H, J = 9.6 Hz), 8.55−8.10 (7H), 8.14 (s, 1H), 8.12 (dd, 1H, J = 9.6, 8.0 Hz), 6.13 (t, 1H, J = 6.6 Hz), 5.23 (br, 1H), 5.10 (br, 1H), 4.44 (d, 2H, J = 5.5 Hz), 4.26−4.21 (m, 1H), 3.64−3.56 (m, 2H), 2.19−2.12 (m, 2H); ^{13}C NMR (DMSO-d_6, 125 MHz) δ = 168.5, 161.8, 149.5, 143.6, 131.7, 131.0, 130.7, 130.1, 128.3, 128.2, 127.9, 127.1, 126.5, 125.8, 125.6, 125.2, 124.6, 124.3, 123.7, 123.6, 98.2, 89.6, 87.6, 84.7, 74.5, 70.2, 61.0, 40.0, 29.4; FABMS (NBA/DMSO), m/z 510 ([M+H]$^+$), HRMS calcd. for $C_{29}H_{24}N_3O_6$ ([M+H]$^+$) 510.1665, found 510.1667.

5-[3-(1-Pyrenylmethylamino)propynyl]-5′-*O*-(4,4′-dimethoxytrityl)-2′-deoxyuridine (2b). To a solution of **1** (523 mg, 0.961 mmol), **5b** (333 mg, 1.24 mmol), and triethylamine (0.530 mL, 3.78 mmol) in 10 mL of anhydrous DMF was added tetrakis(triphenylphosphine)-palladium(0) (492 mg, 0.426 mmol) and copper(I) iodide (162 mg, 0.852 mmol) under nitrogen. The mixture was stirred at room temperature for 12 h. The resulting mixture was concentrated in vacuo and diluted in ethyl acetate. This solution was washed with 5% (w/v) EDTA solution and 5% (w/v) sodium bisulfite solution, dried over Na_2-SO_4, filtered and evaporated. The crude product was purified by silica gel column chromatography (chloroform−methanol = 50:1) yield **2b** (465 mg, 60%) as a white solid: ^{1}H NMR (DMSO-d_6, 400 MHz) δ = 11.70 (s, 1H), 8.45−7.96 (11H), 7.35−7.09 (9H), 6.89−6.75 (4H), 6.13 (t, 1H, J = 6.7 Hz), 5.35 (d, 1H, J = 4.4 Hz), 4.38 (d, 2H, J = 5.7 Hz), 4.31−4.28 (m, 1H), 3.94−3.89 (m, 1H), 3.63 (s, 3H), 3.60 (s, 3H), 3.40 (d, 2H, J = 3.1 Hz), 3.23 (dd, 1H, J = 10.2, 5.0 Hz), 3.07 (dd, 1H, J = 10.2, 2.4 Hz), 2.28 (dt, 1H, J = 13.4, 6.8 Hz), 2.20 (ddd, 1H, J = 13.4, 6.4, 3.6 Hz); ^{13}C NMR (DMSO-d_6, 125 MHz) δ = 161.7, 158.0, 157.9, 149.3, 144.6, 142.5, 135.5, 130.7, 130.3, 130.0, 129.7, 129.6, 129.5, 128.7, 128.6, 127.8, 127.5, 127.4, 127.3, 127.0, 126.8, 126.5, 126.0, 125.0, 124.9, 124.5, 124.1, 123.92, 123.85, 113.2, 113.13, 113.09, 98.8, 86.0, 85.81, 85.80, 85.79, 84.9, 79.1, 75.3, 70.4, 63.6, 54.93, 54.87, 54.86, 49.2, 39.9, 38.0, 37.8; FABMS (NBA/DMSO), m/z 798 ([M+H]$^+$), HRMS calcd. for $C_{50}H_{43}N_3O_7$ ([M+H]$^+$) 798.3179, found 325.1473.

5-[3-(1-Pyrenylmethylamino)propynyl]-5′-*O*-(4,4′-dimethoxytrityl)-2′-deoxyuridine 3′-*O*-(2-cyanoethyl)-*N*,*N*-diisopropylphosphoramidite (3b). To a solution of 2b (48 mg, 60 μmol) and tetrazole (4.9 mg, 71 μmol) in anhydrous acetonitrile (0.6 mL) was added 2-cyanoethyl tetraisopropylphosphorodiamidite (22 μL, 70 μmol) under nitrogen. The mixture was stirred at room temperature for 1 h. The mixture was filtered and used for oligodeoxynucleotide synthesis without further purification.

5-[3-(1-Pyrenylmethylamino)propynyl]-2′-deoxyuridine (4b). To a solution of **2b** (75 mg, 94.1 μmol) in 1 mL of dichloromethane was added 3% trichloroacetic acid in dichloromethane (3 mL) and the mixture was stirred for 5 min at room temperature. The resulting mixture was evaporated and purified by silica gel column chromatography (chloroform−methanol = 50:1) yield **4b** (35 mg, 75%): ^{1}H NMR (CD_3-OD, 400 MHz) δ = 8.51−8.48 (2H), 8.33−8.30 (4H), 8.22−8.08 (4H), 6.23 (t, 1H, J = 6.4 Hz), 5.12 (s, 2H), 4.39 (dt, 1H, J = 6.4, 3.6 Hz), 4.27 (s, 2H), 3.96 (q, 1H, J = 3.6 Hz), 3.80 (dd, 1H, J = 12.0 Hz), 3.72 (dd, 1H, J = 12.0, 3.2 Hz), 2.36 (ddd, 1H, J = 13.6, 6.4, 3.6 Hz), 2.22 (dt, 1H, J = 13.6, 6.4 Hz); ^{13}C NMR (CD_3OD, 125 MHz) δ = 164.5, 151.0, 146.6, 134.0, 132.6, 132.0, 131.2, 130.3, 130.0, 129.8, 127.7, 127.2, 127.0, 126.2, 126.1, 125.6, 123.2, 98.4, 89.4, 87.5, 72.0, 62.5, 58.3, 49.9, 49.5, 49.3, 42.0, 38.3; FABMS (DTT−TG/CH_3OH), m/z 496 ([M+H]$^+$), HRMS calcd. for $C_{29}H_{25}N_3O_5$ ([M+H]$^+$) 496.1868, found 496.1872.

4-*N*-(*N*,*N*-Dimethylaminomethylidenyl)-5-iodo-5′-*O*-(4,4′-dimethoxytrityl)-2′-deoxycytidine (7). To a solution of the 5-iodo-2′-deoxycytidine (**6**, 500 mg, 1.42 mmol) in dry DMF (5 mL) was added *N*,*N*-dimethylformamide dimethylacetal (5.3 mL, 30.0 mmol), and the

solution was stirred at 55 °C for 2 h and concentrated in vacuo. The residue was solved in dry pyridine (5 mL), and then 4,4′-dimethoxytrityl chloride (577 mg, 1.70 mmol) was added. The mixture was stirred at room temperature for 5 h. The mixture was concentrated in vacuo. The crude product was purified by silica gel column chromatography (chloroform−methanol = 20:1) to yield **7** (710 mg, 50%) as a white solid: ^{1}H NMR ($CDCl_3$, 500 MHz) δ = 8.71 (s, 1H), 8.24 (s, 1H), 7.43−7.13 (9H), 6.85−6.80 (4H), 6.30 (t, 1H, J = 6.5 Hz), 4.45 (dt, 1H, J = 6.0, 3.1 Hz), 4.11 (q, 1H, J = 3.4 Hz), 3.77 (s, 6H), 3.38 (dd, 1H, J = 10.4, 3.6 Hz), 3.33 (dd, 1H, J = 10.4, 3.6 Hz), 3.19 (s, 3H), 3.16 (s, 3H), 2.65 (ddd, 1H, J = 13.7, 5.7, 3.1 Hz), 2.19 (dt, 1H, J = 13.6, 6.2 Hz); ^{13}C NMR ($CDCl_3$, 125 MHz) δ = 158.9, 158.63, 158.57, 146.5, 144.5, 139.3, 135.7, 130.09, 139,06, 129.1, 128.1, 128.0, 127.82, 127.75, 127.71, 127.1, 126.9, 113.3, 113.2, 113.0, 87.5, 86.8, 86.2, 81.4, 77.2, 72.3, 63.5, 55.2, 41.4, 35.5; FABMS (DTT−TG/$CHCl_3$), m/z 711 ($[M+H]^+$), HRMS calcd. for $C_{33}H_{36}N_4O_6$ ($[M+H]^+$) 711.1680, found 711.1675.

4-*N*-(*N*,*N*-Dimethylaminomethylidenyl)-5-[3-(1-pyrenecarboxamido)propynyl]-5′-*O*-(4,4′-dimethoxytrityl)-2′-deoxycytidine (8). To a solution of **7** (500 mg, 0.71 mmol), **5a** (191 mg, 0.71 mmol), and triethylamine (0.12 mL, 0.86 mmol) in 7 mL of anhydrous DMF was added tetrakis(triphenylphosphine)palladium(0) (164 mg, 0.142 mmol) and copper(I) iodide (54.1 mg, 0.284 mmol) under nitrogen. The mixture was stirred at room temperature for 12 h. The resulting mixture was concentrated in vacuo and diluted with ethyl acetate. This solution was washed with 5% (w/v) EDTA solution and 5% (w/v) sodium bisulfite solution, dried over Na_2SO_4, filtered and evaporated. The crude product was purified by silica gel column chromatography (chloroform−methanol = 25:1) to yield **8** (291 mg, 47%): ^{1}H NMR (DMSO-d_6, 400 MHz) δ = 9.10 (t, 1H, J = 5.6 Hz), 8.62 (s, 1H), 8.49−8.07 (9H), 7.42−7.19 (9H), 6.90−6.87 (4H), 6.14 (t, 1H, J = 6.4 Hz), 5.38 (d, 1H, J = 4.0 Hz), 4.35−4.31 (m, 1H), 4.27 (d, 2H, J = 5.2 Hz), 3.98−3.95 (m, 1H), 3.693 (s, 3H), 3.685 (s, 3H), 3.29 (dd, 1H, J = 12.0, 4.8 Hz), 3.14 (s, 3H), 3.12−3.09 (m, 1H), 3.04 (s, 3H), 2.30 (ddd, 1H, J = 13.6, 6.4, 3.6 Hz), 2.15 (dt, 1H, J = 13.6, 6.4 Hz); ^{13}C NMR (DMSO-d_6, 125 MHz) δ = 169.9, 168.4, 158.1, 158.0, 157.8, 153.3, 144.7, 144.6, 135.7, 135.2, 131.7, 131.1, 130.7, 130.1, 129.7, 129.6, 128.3, 128.0, 127.9, 127.5, 127.1, 126.62, 126.56, 125.8, 125.6, 125.1, 124.5, 124.3, 123.8, 123.6, 113.24, 113.21, 97.7, 88.9, 85.91, 85.87, 79.1, 75.9, 70.6, 63.7, 55.0, 40.9, 40.8, 34.8, 29.5; FABMS (NBA/DMSO), m/z 866 ($[M+H]^+$), HRMS calcd. for $C_{53}H_{47}N_5O_7$ ($[M+H]^+$) 866.3554, found 866.3550.

4-*N*-(*N*,*N*-Dimethylaminomethylidenyl)-5-[3-(1-pyrenecarboxamido)propynyl]-5′-*O*-(4,4′-dimethoxytrityl)-2′-deoxycytidine 3′-*O*-(2-cyanoethyl)-*N*,*N*-diisopropylphosphoramidite (9). To a solution of 8 (52 mg, 64 μmol) and tetrazole (4.9 mg, 70 μmol) in anhydrous acetonitrile (0.8 mL) was added 2-cyanoethyl tetraisopropylphosphorodiamidite (22 μL, 70 μmol) under nitrogen. The mixture was stirred at room temperature for 1 h. The mixture was filtered and used for oligodeoxynucleotide synthesis without further purification.

Oligodeoxynucleotide (ODN) Synthesis and Characterization. ODNs were synthesized by a conventional phosphoramidite method by using an Applied Biosystems 392 DNA/RNA synthesizer. ODNs were purified by reverse phase HPLC on a 5-ODS-H column (10 × 150 mm, elution with 0.1 M triethylamine acetate (TEAA), pH 7.0, linear gradient over 50 min from 0% to 50% acetonitrile at a flow rate 3.0 mL/min). ODNs containing modified nucleotides were fully digested with calf intestine alkaline phosphatase (50 U/mL), snake venom phosphodiesterase (0.15 U/mL), and P1 nuclease (50 U/mL) at 37 °C for 3 h. Digested solutions were analyzed by HPLC on a CHEMCOBOND 5-ODS-H column (4.6 × 150 mm), elution with a solvent mixture of 0.1 M triethylamine acetate (TEAA), pH 7.0, flow rate 1.0 mL/min). Concentration of each ODN was determined by comparing peak areas with standard solution containing dA, dC, dG, and dT at a concentration of 0.1 mM. **ODN1(^{Py}U)** 5′-d(CGCAAT^{Py}UTAACGC)-3′: ESI-TOF [$(M-3H)^{3-}$] calcd 1394.24, found 1394.17. **ODN1($^{Py(amino)}$U)** 5′-d(CGCAAT$^{Py(amino)}$UTAACGC)-3′: MALDI-TOF [$(M-H)^-$] calcd 4170.88, found 4170.79. **ODN2(^{Py}U)** 5′-d(CGCAAC^{Py}UCAACGC)-3′: ESI-TOF [$(M-3H)^{3-}$] calcd 1384.13, found 1384.28. **ODN2(^{Py}C)** 5′-d(CGCAAC^{Py}CCAACGC)-3′: ESI-TOF [$(M-5H)^{5-}$] calcd 829.96, found 827.57. **ODN_{ras}(^{Py}U)** 5′-d(GGCGCCG^{Py}UCGGTGTG)-3′: ESI-TOF [$(M-3H)^{3-}$] calcd 1635.09, found 1636.59. **ODN_{BRCA2}(^{Py}C)** 5′-d(GCAGCCT^{Py}CAGGCAGC)-3′: ESI-TOF [$(M-4H)^{4-}$] calcd 806.37, found 804.01.

Melting Temperature (T_m) Measurements. All T_ms of the ODNs (2.5 μM, final duplex concentration) were taken in 50 mM sodium phosphate buffers (pH 7.0) containing 100 mM sodium chloride. Absorbance vs temperature profiles were measured at 260 nm using a Shimadzu UV-2550 spectrophotometer equipped with a Peltier temperature controller using 1 cm path length cell. The absorbance of the samples was monitored at 260 nm from 5 °C to 90 °C with a heating rate of 1 °C/min. From these profiles, first derivatives were calculated to determine T_m values.

UV Absorption Measurements. ODN solutions were prepared as described in T_m measurement experiment. Absorption spectra were obtained using an Ultraspec 3000pro UV−vis spectrophotometer (Amarsham Pharmacia Biotech) at room temperature using 1 cm path length cell.

Fluorescence Experiments. ODN solutions were prepared as described in T_m measurement experiment. Fluorescence spectra were obtained using a Shimadzu RF-5300PC spectrofluorophotometer at 25 °C using 1 cm path length cell. The excitation bandwidth was 1.5 nm. The emission bandwidth was 1.5 nm.

The fluorescence quantum yields (Φ_F) were determined using 9,10-diphenylanthracene as a reference with a known Φ_F of 0.95 in ethanol.[6] The area of the emission spectrum was integrated using the software available in the instrument, and the quantum yield is calculated according to the following equation

$$\Phi_{F(S)}/\Phi_{F(R)} = [A_{(S)}/A_{(R)}] \times [(Abs)_{(R)}/(Abs)_{(S)}] \times [n_{(S)}^2/n_{(R)}^2] \quad (1)$$

Here, $\Phi_{F(S)}$ and $\Phi_{F(R)}$ are the fluorescence quantum yield of the sample and the reference, respectively. $A_{(S)}$ and $A_{(R)}$ are the area under the fluorescence spectra of the sample and the reference, respectively, $(Abs)_{(S)}$ and $(Abs)_{(R)}$ are the respective optical densities of the sample and the reference solution at the wavelength of excitation, and $n_{(S)}$ and $n_{(R)}$ are the values of refractive index for the respective solvents used for the sample (1.333) and the reference (1.383).

Fluorescence imaging was performed using Bio-Rad VersaDoc 3000. The sample solution was illuminated with a 290−365 nm transilluminator. Image was taken through a 380-nm long pass emission filter.

JA039625Y